THE JOURNAL OF NAVIGATION (2005), **58**, 375–388. © The Royal Institute of Navigation
doi:10.1017/S037346330500336X Printed in the United Kingdom

On Navigation Systems for Motorcycles: The Influence and Estimation of Roll Angle

Joshua P. Coaplen, Patrick Kessler, Oliver M. O'Reilly, Dan M. Stevens and J. Karl Hedrick

(*Department of Mechanical Engineering*, *University of California*)
(Email: oreilly@berkeley.edu)

Vehicle navigation systems use various sensors and the global positioning system (GPS) to locate a vehicle. This location is then matched to a map database to provide navigation information. Between GPS updates, the vehicle's heading angle and forward speed are used to "dead reckon" its position. Heading angle is often measured by integrating the output of a rate gyroscope. For this measurement to be equal to the vehicle's heading angle, the vehicle should not experience any rotation about its roll or pitch axes. For an automobile, the roll and pitch angles are small and may be neglected for the purposes of navigation. This article demonstrates that this same assumption is not true for a motorcycle. Through simulation, it is shown that for a motorcycle, obtaining a meaningful heading angle from a single angular rate measurement requires accounting for the motorcycle's roll angle. Methods to estimate roll angle and heading angle from available navigation measurements are presented, and two possible sensor configurations are compared. A motorcycle navigation scheme based on these roll angle estimation methods is shown to produce exceptional results in a simulation environment.

KEY WORDS

1. Motorcycle. 2. Navigation. 3. Dead-reckoning. 4. GPS.

1. INTRODUCTION. Modern ground-vehicle navigation systems use various sensors, the global positioning system (GPS), and geographic information systems (GIS) to determine the position of a vehicle (El-Rabbany, 2002). It is well known that GPS alone is usually inadequate for ground-vehicle navigation because of loss or obstruction of signals in certain operating environments (urban canyons, heavy tree cover, tunnels, parking structures, etc.) and, to a lesser degree, slow update rates (Farrell and Barth, 1999; Turetzky *et al.*, 1998; El-Rabbany, 2002). To improve system robustness in such environments, a terrestrial navigation system is used in addition to GPS. The terrestrial navigation system provides "continuous" position estimates, which are typically combined with GPS updates in a complementary filter arrangement to provide navigation information regardless of GPS availability (Farrell *et al.*, 2000). This navigation information is then

https://doi.org/10.1017/S037346330500336X Published online by Cambridge University Press

compared with the GIS for final output to the user. Such navigation systems are known as GPS-aided systems and are widely available on the automotive market, both as OEM (Original Equipment Manufacturer) equipment and aftermarket accessories.

Automotive terrestrial navigation systems generate position estimates from sensors using deduced reconnaissance, more commonly known as "dead reckoning" (Biezad, 1999; El-Rabbany, 2002). In comparison, current motorcycle navigation systems rely solely on GPS, rendering them useless when GPS updates are unavailable or corrupted. This article investigates the additional requirements of a dead reckoning system for a motorcycle as compared to those for a 4-wheeled vehicle. Specifically, we study the possibility of using or modifying an "off the shelf" dead reckoning system developed for an automobile to provide accurate dead reckoned motorcycle position estimates without the need for additional hardware. The motivation is that given a suitable motorcycle dead reckoning system, the more general problem of robust motorcycle navigation is effectively solved in a manner identical to the robust automotive navigation problem.

This paper is organized as follows: Section 2 gives some background on existing dead reckoning systems and their applicability to motorcycles. Parameterization of vehicle orientation is discussed in section 3 as a segue into the fundamental differences between automotive and motorcycle dead reckoning systems in section 4 and the effects of ignoring these differences in section 5. Section 6 gives a novel model-based method of estimating motorcycle roll angle, which is validated against experimental and simulation results. Finally, in section 7, a motorcycle dead reckoning system is presented which requires no additional hardware compared to a similar automotive system. In a forthcoming sequel to this paper, the proposed system is demonstrated using data from a motorcycle.

2. BACKGROUND.

Dead reckoning of a ground-based vehicle provides relative planar position in a navigation plane[1] using time and a vehicle's heading angle and speed as inputs (O'Donnell, 1964). Since most ground-based vehicles come equipped with the ability to measure forward speed and time, dead-reckoning an automobile usually only requires the addition of the sensor(s) needed to determine the heading angle[2]. For example, equation (1) determines the planar location $\mathbf{r} = x\mathbf{E_1} + y\mathbf{E_2}$ of a point on the vehicle using a measure of the vehicle's forward speed $u(t)$ and the heading angle η (see Figure 1):

$$\begin{aligned} x(t_1) &= x(t_0) + \int_{t_0}^{t_1} u(\tau)\cos(\eta)d\tau, \\ y(t_1) &= y(t_0) + \int_{t_0}^{t_1} u(\tau)\sin(\eta)d\tau. \end{aligned} \tag{1}$$

[1] The navigation plane is locally tangent to the Earth at the point occupied by the vehicle.

[2] The heading angle η in (1) is defined by the SAE to be, "the horizontal angle between a reference line fixed in the vehicle and a reference line fixed in the roadway, giving a measure of vehicle yaw rotation or directional orientation relative to the roadway" (Anon, 1976). This definition becomes ambiguous when the vehicle rolls or pitches as described in section 3.

https://doi.org/10.1017/S037346330500336X Published online by Cambridge University Press

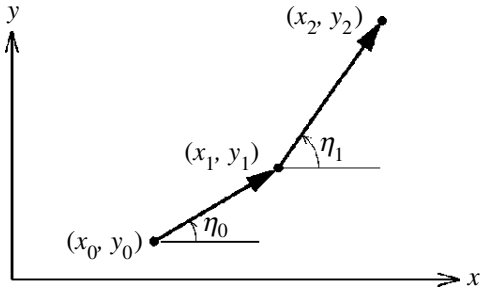


Figure 1. Dead reckoning through two steps of input data. Although (1) is continuous in time, in applications a discretized version as illustrated in this figure is used: $s_i = \int_{t=i}^{t=i+1} u(\tau)d\tau$, $\eta_i = \int_{t=i}^{t=i+1} \dot{\eta}d\tau$ (see (Kao, 1991)).

Many methods of obtaining heading angle exist for automotive (4-wheeled vehicles) navigation systems, with new and more accurate methods being continually developed. For a state of the art example, see (Yang and Farrell, 2003). Popular methods currently used in commercial applications are (Heckermann *et al*., 1997; El-Rabbany, 2002):

1. Integrating the output of an angular rate sensor aligned with the yaw axis of the automobile;
2. Sensing the difference in rotation between left and right wheels;
3. Using a compass (magnetic field sensor).

For example, as of 1997 the OEM navigation system for the BMW 5-Series automobiles used a compass and automatic stability control (ASC) speed sensors (Heckermann *et al*., 1997). Alternatively, several aftermarket navigation systems use only an angular rate sensor. For a motorcycle, the options for sensing heading angle are fewer, since any method requiring comparisons between the left and right sets of wheels is not possible.

Use of angular rate sensors for establishing vehicle heading angle is common in vehicle applications, both because of low cost and ease of implementation (El-Rabbany, 2002). In such applications, the angular rate sensor remains in the body frame, that is, it is rigidly attached to the vehicle. Consequently, for the measured angular rate to correspond well with the vehicle's actual heading rate, the vehicle should not experience any rotation about the roll and/or pitch axes. For a 4-wheeled vehicle, the roll and pitch angles during operation are small and are typically neglected, i.e., no corrections are made for the difference between the measured angular rate (yaw) axis and local vertical (navigation plane normal). However, compared to an automobile, the roll angle experienced by a motorcycle can become large, resulting in significant deviations of the measured angular rate axis from the local vertical. As is shown in Section 5, for motorcycles, large inaccuracies in position predictions are generated by ignoring the effect of vehicle roll.

It is in the determination of the angle η that dead reckoning for single track vehicles differs from 4-wheeled vehicles. Section 4 details the differences. However, given η, dead reckoning a motorcycle is identical to dead reckoning an automobile.

https://doi.org/10.1017/S037346330500336X Published online by Cambridge University Press

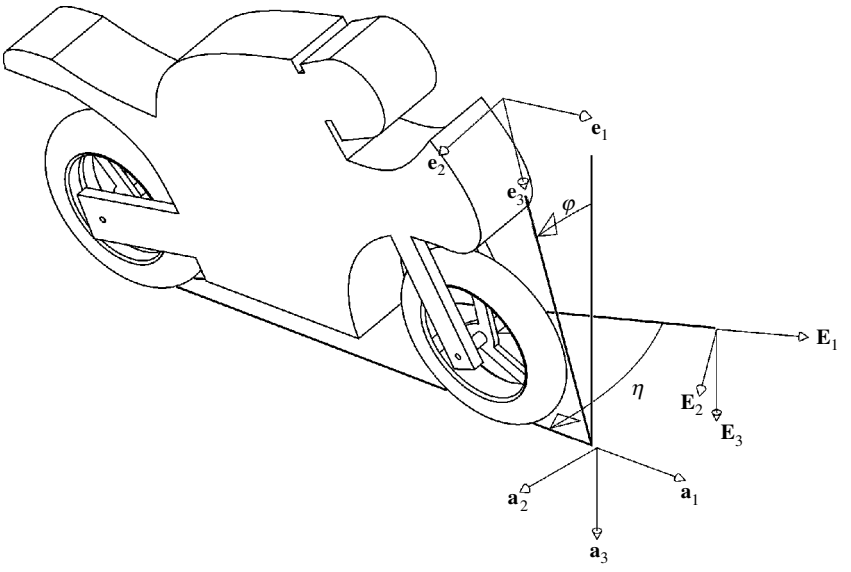


Figure 2. The body fixed axes $\{\mathbf{e}_1,\mathbf{e}_2,\mathbf{e}_3\}$ for a motorcycle. These axes correspond to the SAE vehicle axes $\{\mathbf{x},\mathbf{y},\mathbf{z}\}$: roll, pitch, and yaw respectively.

3. ORIENTATION OF A SINGLE TRACK VEHICLE. The orientations considered are those of a rigid body which models either the frame of a motorcycle or the sprung mass of an automobile. In both cases, $\{\mathbf{e}_i\}$ denote a set of basis vectors fixed to the body.

The angular velocity of the body can be written with respect to the $\{\mathbf{e}_i\}$ basis as

$$\omega = \omega_1\mathbf{e}_1 + \omega_2\mathbf{e}_2 + \omega_3\mathbf{e}_3 \tag{2}$$

where ω_1, ω_2, and ω_3 are known according to the SAE convention as roll velocity, pitch velocity, and yaw velocity respectively (Anon, 1976). Three angles are now defined to parameterize the orientation of the vehicle[3]. For convenience, the angles are chosen to correspond to angles with physical significance and describe the relative orientations of three right-handed, orthonormal triads (see Figure 2). The first triad, $\{\mathbf{E}_1, \mathbf{E}_2, \mathbf{E}_3\}$ is Earth-fixed, while the second, $\{\mathbf{e}_1, \mathbf{e}_2, \mathbf{e}_3\}$ is fixed to the frame of the motorcycle (or the sprung mass of the automobile). The frame $\{\mathbf{e}_i\}$ can be obtained by three successive rotations of the $\{\mathbf{E}_i\}$ frame:

1. Rotate about the $\mathbf{E}_3$ axis through the angle η (this yields the $\{\mathbf{a}_i\}$ frame in Fig. 2)
2. Rotate about the $\mathbf{a}_2$ axis through the angle α (this frame is not shown in Fig. 2)
3. Rotate about the $\mathbf{e}_1$ axis through the angle φ.

This sequence of rotations can be concisely expressed as

$$\begin{bmatrix}\mathbf{a}_1\\ \mathbf{a}_2\\ \mathbf{a}_3\end{bmatrix} = \begin{bmatrix}\cos(\eta) & \sin(\eta) & 0\\ -\sin(\eta) & \cos(\eta) & 0\\ 0 & 0 & 1\end{bmatrix}\begin{bmatrix}\mathbf{E}_1\\ \mathbf{E}_2\\ \mathbf{E}_3\end{bmatrix}, \tag{3}$$

[3] The presented parameterization of orientation is equivalent to the 3-2-1 set of Euler angles.

https://doi.org/10.1017/S037346330500336X Published online by Cambridge University Press

$$\begin{bmatrix} \mathbf{e}_1 \\ \mathbf{e}_2 \\ \mathbf{e}_3 \end{bmatrix} = \begin{bmatrix} \cos(\alpha) & 0 & -\sin(\alpha) \\ \sin(\varphi)\sin(\alpha) & \cos(\varphi) & \sin(\varphi)\cos(\alpha) \\ \cos(\varphi)\sin(\alpha) & -\sin(\varphi) & \cos(\varphi)\cos(\alpha) \end{bmatrix} \begin{bmatrix} \mathbf{a}_1 \\ \mathbf{a}_2 \\ \mathbf{a}_3 \end{bmatrix}. \tag{4}$$

Note that the angular velocity can also be written in terms of $\dot{\eta}$, $\dot{\alpha}$, and $\dot{\varphi}$ as

$$\omega = \dot{\eta}\mathbf{E}_3 + \dot{\alpha}\mathbf{a}_2 + \dot{\varphi}\mathbf{e}_1. \tag{5}$$

Setting (2) equal to (5), and using (3) and (4), the following relationships are obtained:

$$\begin{aligned} \omega_1 &= -\dot{\eta}\sin(\alpha) + \dot{\varphi}, \\ \omega_2 &= \dot{\eta}\sin(\varphi)\cos(\alpha) + \dot{\alpha}\cos(\varphi), \\ \omega_3 &= \dot{\eta}\cos(\varphi)\cos(\alpha) - \dot{\alpha}\sin(\varphi). \end{aligned} \tag{6}$$

The Society of Automotive Engineers (SAE) attaches the names *heading*, *pitch*, and *roll* to the angles η, α, and φ respectively. Notice that according to (6), in general $\dot{\eta} \neq \omega_3$, $\dot{\alpha} \neq \omega_2$, and $\dot{\varphi} \neq \omega_1$, which, in words, means the time rate of change of pitch angle does not equal the pitch velocity, the time rate of change of roll angle does not equal the roll velocity, and so on.

A common assumption in automotive navigation systems is that the pitch angle is negligible, that is, $\alpha \approx 0$. It is reasonable to invoke this same assumption for single-track vehicles[4]. Enforcing the zero pitch constraint means the $\mathbf{e}_1$ axis will remain in the $\{\mathbf{E}_1, \mathbf{E}_2\}$ plane. Setting $\alpha \approx 0$ in (6) and rearranging gives the following differential equations:

$$\dot{\varphi} = \omega_1, \tag{7}$$

$$\dot{\eta} = \sec(\varphi)\omega_3, \tag{8}$$

$$\omega_2 = \tan(\varphi)\omega_3. \tag{9}$$

Thus, when pitch is neglected, integration of the system of differential equations given by (7) and (8) will yield the orientation of the motorcycle[5] while (9) is the constraint representing the zero pitch condition. The quantities ω_1 in (7) and ω_3 in (8) are those that would be measured by angular rate sensors fixed to the motorcycle frame and aligned with the roll and yaw axes respectively.

4. PRESCRIPTIONS FOR HEADING ANGLE. For a typical 4-wheeled vehicle, it is common to assume that the only non-negligible orientation angle is the heading angle η. In such a case, when both pitch and roll are neglected ($\alpha \approx 0$, $\varphi \approx 0$), the yaw rate gyro, ω_3, provides the heading angle after a single integration of (8):

$$\eta(t) = \eta(0) + \int_0^t \omega_3 d\tau. \tag{10}$$

[4] When using the motorcycle model proposed by (Cossalter *et al.*, 1999), if the front and rear tyres have identical dimensions, the zero pitch constraint is analogous to requiring that the two tyres remain in contact with the road.

[5] With the zero pitch constraint, the same system of equations is obtained by using either the 3-1-2 or 2-3-1 Euler angle parameterizations.

https://doi.org/10.1017/S037346330500336X Published online by Cambridge University Press

This simple equation is a key component of dead-reckoning systems in automobiles. Unfortunately, when the roll angle deviates significantly from zero, (10) does not represent a physical angle of rotation. This was first pointed out by Goodman and Robinson (1952)[6] who noted that when the axis of rotation is not fixed, blind integration of body-fixed rate sensors to provide angles of rotation is meaningless and a source of drift in inertial navigation systems.

Like 4-wheeled vehicles, the pitch angle of a single track vehicle is typically small enough to be negligible ($\alpha \approx 0$). However, unlike 4-wheeled vehicles, the roll angle φ of a single track vehicle does not remain small during general operation. Consequently, from (8), when roll angle is not negligible the heading angle is given by

$$\eta(t) = \eta(0) + \int_0^t \sec(\varphi)\omega_3 \, d\tau. \tag{11}$$

Thus, in contrast to (10) where heading angle can be determined from a single input, determination of the heading angle from (11) requires two inputs: yaw velocity ω_3 and roll angle φ. This suggests that a dead-reckoning system in a motorcycle requires supplemental information when compared to the same system in an automobile. To obtain this supplemental information, one could use hardware (such as another rate gyroscope to measure ω_1), or develop a method of estimating φ without the need for additional hardware. Alternatively, one could ignore the effect of roll entirely in hopes that the $sec(\varphi)$ term in (8) remains close enough to unity to be ignored. In light of the later possibility, it is prudent to examine the significance of roll angle in determining heading angle.

5. ROLL ANGLE'S INFLUENCE ON POSITION ESTIMATION.

In Section 4 two prescriptions for heading angle were presented: (10) and (11). Both prescriptions assume that pitch is zero, and one of them, (10), also assumes that roll is zero. It will be demonstrated through simulation that ignoring the roll angle in a dead-reckoning algorithm for a single-track vehicle can lead to large errors in position estimates.

To examine the effects of neglecting roll angle, an ADAMS motorcycle model, hereafter referred to as "the ADAMS model", was developed for simulation. The details and development of this model can be found in (Stevens, 2002). Simulations were performed in which the motorcycle negotiated a typical city block (see Figure 3). The city block in Figure 3 is 200 metres on each side, with a turn radius of 6 metres. The motorcycle moved around the block at a constant speed and reached a maximum roll angle φ of about 25°. The solid line denotes the actual position of a point of the motorcycle. The dashed line denotes the dead-reckoned position, where the heading angle was determined using (10), and the speed was determined by assuming that the front wheel of the motorcycle was rolling without slipping[7]. The third set of results, which are indistinguishable from the solid line, used (11) to determine heading angle, with speed determined as in the previous case. After each turn, there is about a 10°

[6] Goodman and Robinson's remarks are interpreted in the modern literature in terms of geometric phases (see, for example, Marsden and Ratiu (1994) or O'Reilly (1997)).

[7] This is the usual method by which the speedometer reading is obtained from the rotation speed of the front wheel of the motorcycle.

https://doi.org/10.1017/S037346330500336X Published online by Cambridge University Press

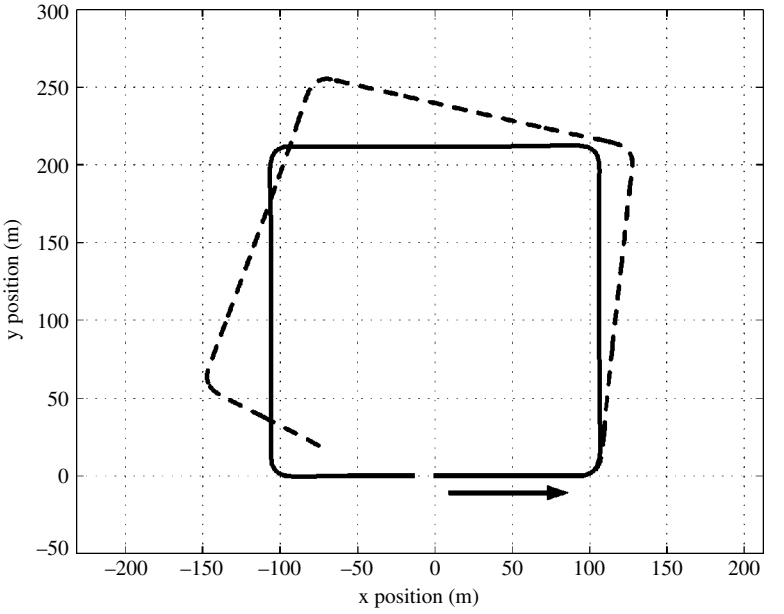


Figure 3. Simulations of a motorcycle's position as it moves around a city block at a constant speed.

difference accumulated between the actual heading and the direction given by (10). By the end of the block, ignoring roll angle during dead reckoning of a motorcycle (that is using (10) instead of (11)) yields significantly erroneous position information.

Figure 4 shows results of simulating a motorcycle through a 90° turn. The path for the turn consists of the arc of a circle with a radius of 61m. As in Figure 3, motorcycle speed was held constant through the turn for each value of roll angle. Results for various roll angles were generated by increasing speed. As expected from (10) and (11), heading error[8] increased with increasing roll angle. Note that heading angle error is a result of an integration through time, so increased roll angles and increased time in a turn will both result in increased heading error. The effect of ignoring roll angle is clear; for realistic motorcycle manoeuvres, heading angle error can accumulate to the point of making position estimates by dead reckoning unusable for navigation purposes. Methods for correcting for roll angle are now discussed.

6. ESTIMATING ROLL. Section 5 demonstrated the effect of roll angle on obtaining an accurate heading angle, and consequently on obtaining an accurate position estimate. In the planar case (i.e., when the pitch angle is neglected), the heading rate is a function of the cosine of the roll angle and ω_3, as shown in (8). Given access to the roll angle of the motorcycle, one could account for its effect on the position estimate.

Possibly the most obvious solution is to measure the roll angle directly, by using a rate gyro aligned with the roll axis $\mathbf{e}_1$, or by using some other sensor. This, along with

[8] Heading error = actual heading angle $-\int \omega_3 dt$.

https://doi.org/10.1017/S037346330500336X Published online by Cambridge University Press

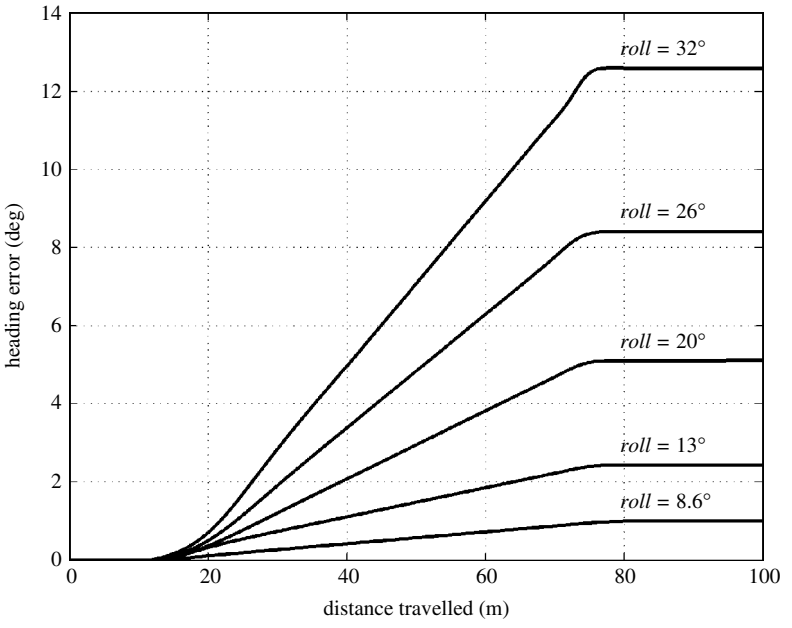


Figure 4. Heading error (actual heading angle $-\int \omega_3 dt$) accumulated during a single 90° turn. Motorcycle speed was increased to increase the roll angle and turning radius is 61 m. The x-axis label refers to the distance travelled in the $\mathbf{E}_1$ direction assuming the $\{\mathbf{e}_i\}$ frame was aligned with the $\{\mathbf{E}_i\}$ frame at $t=0$.

a rate gyro aligned with the yaw axis $\mathbf{e}_3$, allows for the computation of (11). Of course, adding another sensor increases cost and introduces additional measurement error. Another option is to obtain roll angle using a dynamic-model-based state observer that uses only the yaw rate and speed as inputs. Some effort was made to pursue this, but establishing observability results for the ADAMS model proved to be prohibitively difficult, both due to the nonlinearities and high system order. Consequently, an approach similar to that of using a dynamic-model-based observer but containing no dynamics in the model was implemented. Effectively, an infinite gain controller (the rider) is assumed to be acting (based on the values of sensor output) to force the motorcycle (and thus the model) to follow the predetermined *natural* condition of steady turning[9]. According to Sharp (2001), "In steady turning, the forward speed and the yaw rate imply a lateral acceleration and a lean angle (for balance in roll to be maintained)." That is, during a steady turn condition, there exists some function f_1 such that $\varphi = f_1(v, \omega_3)$. Of course, the form of this function depends on the model used to describe the motorcycle during a steady turn. Nevertheless, since commercially available automotive navigation systems usually use forward speed v and ω_3 from a yaw rate gyro as inputs, the functional form $\varphi = f_1(v, \omega_3)$ is ideally suited for estimation of φ from available measurements. This eliminates the need for additional sensors, keeping the cost of the motorcycle navigation system to a minimum and decreasing necessary modifications to existing navigation systems.

[9] Steady turning implies constant yaw rate and forward speed (Sharp, 2001).

https://doi.org/10.1017/S037346330500336X Published online by Cambridge University Press

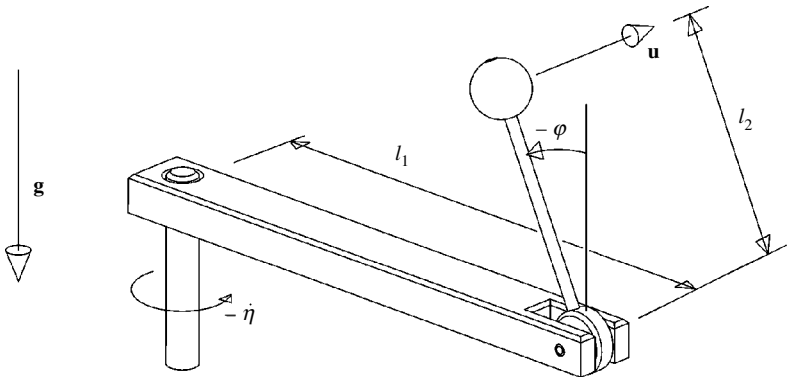


Figure 5. Schematic of the inverted pendulum that is used to motivate the roll angle estimator (13)–(14).

A variety of dynamical systems can be proposed to give form to the desired function $\varphi = f_1(v, \omega_3)$. As a first approximation, a motorcycle executing a steady turn might be sufficiently modelled as an inverted point-mass pendulum, as shown in Figure 5.

A simple relationship exists between ω_3, v, and φ for steady motions ($\ddot{\eta} = \dot{\varphi} = \dot{v} = 0$) of this system[10]:

$$sin(\varphi) = \lambda \frac{v\omega_3}{g} \tag{12}$$

where $\lambda = 1$ for the pendulum and g is acceleration due to gravity[11].

Since a motorcycle in a steady turning condition is not likely to behave exactly as a whirling inverted pendulum, the calibration constant λ is introduced to allow for tuning. Because of the form of (8), it is convenient to find the function f instead of f_1 where

$$cos(\varphi) = f(\lambda, v, \omega_3). \tag{13}$$

Using (12), f can be expressed explicitly as:

$$f = \left(\sqrt{1 - \lambda^2 \left(\frac{v\omega_3}{g} \right)^2} \right). \tag{14}$$

Zellner and Weir (1978) provide experimental data from motorcycles in steady turn conditions. Table 1 is a partial reproduction of their data along with the roll angle predicted from (14) with $\lambda = 1$. As can be seen, the roll estimated by (14) agrees remarkably well with experimental data. This is not entirely surprising based on the observations made by Zellner and Weir that during testing, "For the expert rider, and experienced rider in general, there was negligible body lean relative to the plane of symmetry of the motorcycle … the lateral acceleration, measured by the body fixed accelerometer, is essentially zero in a coordinated turn." The experiments performed

[10] To derive (12), identify $\omega_3 = \dot{\eta} \cos(\varphi)$. Also note that the speed of the mass particle $u = L\dot{\eta}$, where $L = l_1 + l_2 \sin(\varphi)$(the horizontal distance of the mass particle from the axis of rotation).

[11] Equation (12) may be familiar as it is also used to describe a coordinated turn of an airplane (Stevens and Lewis, 1992).

https://doi.org/10.1017/S037346330500336X Published online by Cambridge University Press

Table 1. Roll angles for steady state turns. The experimental data, in ( ), are from (Weir and Zellner, 1978). The predicted data, in [ ], are obtained using (13) and (14), with $\lambda = 1$.

	Path Radius (m)				
Speed (km/h)	7·6	15·2	30·5	61	121·9
16·1	(15°) [14·97°]	(7°) [7·61°]	–	–	–
32·2	–	(28°) [28·13°]	(15°) [14·97°]	–	–
48·3	–	–	(31°) [31·03°]	(17°) [16·74°]	–
64·4	–	–	–	(28°) [28·13°]	(15°) [14·97°]
80·5	–	–	–	(40°) [39·88°]	(23°) [22·67°]
96·6	–	–	–	–	(32°) [31·03°]
112·7	–	–	–	–	(39°) [39·31°]

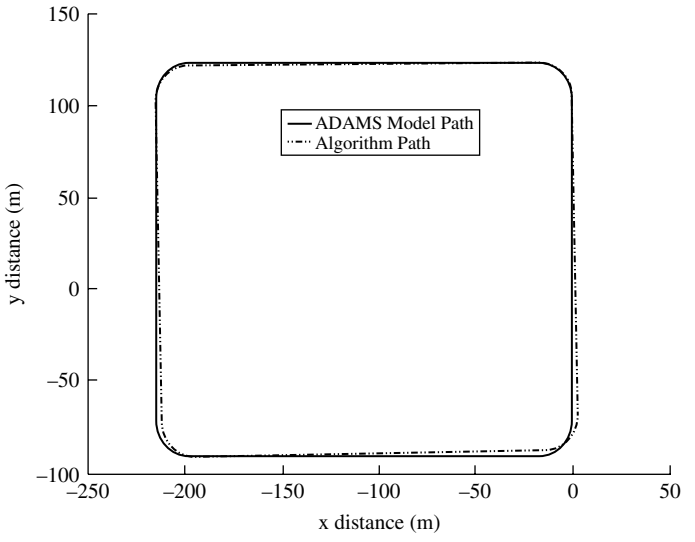


Figure 6. Comparison of the path predicted by the ADAMS model (solid line) and that predicted using the roll angle estimator, (13) and (14), (dashed line) for a particular path of the motorcycle.

by Zellner and Weir show that, when turning, an experienced motorcycle rider will provide the control input necessary to approach a coordinated turn. Furthermore, based on the results in Table 1, (14) is a good model of a motorcycle in a coordinated turn condition for turns of radii 120 m and less.

Simulation further justifies the above claim. Figure 6 shows a path prediction comparison between the ADAMS model and the dead reckoning scheme (2) using the roll angle estimator (14) in (11). The agreement between the two paths justifies the use of (14) to estimate roll angle in (11).

Despite the demonstrated utility of (14) for roll angle estimation, several modifications to the pendulum model were studied in an attempt to more closely model a motorcycle during a turn (see (Kessler, 2004) and (Jutkowitz, 2003)). None of the modified models offered significant improvement over the simple inverted pendulum model in terms of path prediction capability. This conclusion was reached

https://doi.org/10.1017/S037346330500336X Published online by Cambridge University Press

by comparing dead reckoned path results using roll angle estimators derived from the modified models to paths generated using simulation of the ADAMS model.

7. CHOOSING BETWEEN SENSOR ORIENTATIONS. It was shown in Section 6 that roll compensated dead reckoning can be accomplished using only one rate sensor, a measure of speed, and a roll angle estimator such as (14). Although automotive applications usually orient the rate sensor with the yaw axis of the vehicle, this is not necessary for a motorcycle. For instance, the development in Section 6 could have been based on the assumption that the rate sensor was aligned with the roll axis of the bike. The appropriate functional relationship in this case is $\omega_3 = f_2(v,\varphi)$ instead of $\varphi = f_1(v,\omega_3)$. Using the inverted pendulum model (Figure 5 and the relationship $\dot{\eta} = sec(\varphi)\omega_3$), the steady turn condition yields:

$$\dot{\eta} = \begin{cases} \dfrac{g\ tan(\varphi)}{\lambda v} & when\ v \neq 0 \\ 0\ otherwise \end{cases} \tag{15}$$

In contrast, the formulae (14) and (13) from Section 6 combined with $\dot{\eta} = sec(\varphi)\dot{\psi}$ yields:

$$\dot{\eta} = \left(\sqrt{1 - \lambda^2 \left(\frac{v\omega_3}{g} \right)^2} \right)^{-1} \omega_3. \tag{16}$$

Both (15) and (16) use the inverted pendulum model and the assumption of steady turning to estimate heading rate using the input from a single rate gyro and a speedometer. Equation (16) depends directly on an input signal (ω_3) while (15) depends on the integral of an input signal $\left(\varphi = \int_0^t \dot{\phi} d\tau\right)$. From a hardware standpoint, the two methods are identical since they both require one angular rate sensor. However, (16) will achieve more reliable heading estimates in applications because of the required integration in (15) to obtain $\dot{\eta}$ from the rate gyro input. To show this, assume that the speedometer signal is perfect (since this signal is required in both (15) and (16)), while the rate signals and are modelled as

$$\begin{aligned} \omega_3 &= \hat{\dot{\psi}} = \dot{\psi} + \delta\dot{\psi} \\ \omega_1 &= \hat{\dot{\phi}} = \dot{\phi} + \delta\dot{\phi} \end{aligned} \tag{17}$$

where $\hat{\dot{\psi}}$ and $\hat{\dot{\phi}}$ are the signals available to the navigation system, $\dot{\psi}$ and $\dot{\phi}$ are the actual rates, and $\delta\dot{\psi}$ and $\delta\dot{\phi}$ represent the total error in the rate signals from all contributions; noise, misalignment, sensor error, etc. To use (15), the integral of $\hat{\dot{\phi}}$ is needed:

$$\hat{\phi}(t) - \hat{\phi}(t_0) = \int_{t_0}^{t} \hat{\dot{\phi}} d\tau = \int_0^t (\dot{\phi} + \delta\dot{\phi}) d\tau = \phi(t) - \phi(t_0) + \int_0^t \delta\dot{\phi} d\tau. \tag{18}$$

Assuming the initial conditions $\hat{\phi}(t_0)$ and $\phi(t_0)$ are equal, equations (15) and (16) can be expressed respectively as

$$\hat{\dot{\eta}} = \frac{g tan\hat{\phi}}{\lambda v} = \frac{g}{\lambda v} tan\left(\phi + \int_0^t \delta\dot{\phi} d\tau \right) = g_1 \left(\phi + \int_0^t \delta\dot{\phi} d\tau \right) \tag{19}$$

https://doi.org/10.1017/S037346330500336X Published online by Cambridge University Press

and

$$\hat{\dot{\eta}} = \left(\sqrt{1 - \lambda^2 \left(\frac{v\hat{\dot{\psi}}}{g} \right)^2} \right)^{-1} \hat{\dot{\psi}} = g_2(\dot{\psi} + \delta\dot{\psi}). \tag{20}$$

To study the propagation of measurement error through (15) and (16), it is assumed that $\delta\dot{\psi}$ and $z = \int_0^t \delta\dot{\phi} dt$ are small. This allows (19) and (20) respectively to be expanded into Taylor series about the nominal measurements as follows:

$$\hat{\dot{\eta}} = g_1(\phi) + \frac{\partial g_1(\phi)}{\partial \phi} \int_0^t \delta\dot{\phi} d\tau + h.o.t. = \dot{\eta} + \frac{\partial g_1(\phi)}{\partial \phi} \int_0^t \delta\dot{\phi} d\tau + h.o.t. \tag{21}$$

and

$$\hat{\dot{\eta}} = g_2(\dot{\psi}) + \frac{\partial g_2}{\partial \dot{\psi}} \delta\dot{\psi} + h.o.t. = \dot{\eta} + \frac{\partial g_2}{\partial \dot{\psi}} \delta\dot{\psi} + h.o.t. \tag{22}$$

where "h.o.t." represents higher order error terms. Now by defining the error in the heading rate as $\delta\dot{\eta} = \hat{\dot{\eta}} - \dot{\eta}$, (21) and (22) can be written to first order as

$$\delta\dot{\eta} = \frac{\partial g_1(\phi)}{\partial \phi} \int_0^t \delta\dot{\phi} d\tau \tag{23}$$

and

$$\delta\dot{\eta} = \frac{\partial g_2}{\partial \dot{\psi}} \delta\dot{\psi}. \tag{24}$$

According to (23), the error in heading rate when using (15) is $0(t)$, that is, it grows linearly with time. By (24), the error in heading rate when using (16) is $0(t^0)$, it has no structured growth in time. Thus, a motorcycle dead reckoning system based on (16) will be less sensitive to measurement error and consequently more accurate.

8. CONCLUSION. Constructing a dead-reckoning system for a motorcycle has additional demands compared to constructing a similar system for use in a 4-wheeled vehicle. Specifically, ignoring the roll of a motorcycle (as is usually done in 4-wheeled vehicles) was shown through simulation to result in large errors in position estimates. To account for the roll angle during motorcycle manoeuvres, a static model-based estimator was presented based on the assumption that the motorcycle/rider system executes coordinated turns. The estimator was validated through comparison to simulation data.

Using the proposed estimator, a dead reckoning system for a motorcycle requires input from a speedometer and a single angular rate sensor, the same sensor package used by several existing automobile navigation systems. Two orientations of the angular rate sensor will yield appropriate output for navigation. It was shown by studying the propagation of measurement error that the rate sensor should be aligned with the yaw axis of the motorcycle as opposed to the roll axis. Such an arrangement is identical to the arrangement employed by automobile applications. Consequently,

https://doi.org/10.1017/S037346330500336X Published online by Cambridge University Press

existing automotive navigation systems that rely on yaw rate and vehicle speed can be modified, without requiring additional hardware, for use on motorcycles while maintaining a similar level of accuracy in position estimates.

To study the validity of the proposed estimator-based INS system, implementation on a motorcycle is currently underway. Future tests will investigate the accuracy of the proposed system and implementation issues that are not addressed in the theoretical development contained in this article.

ACKNOWLEDGEMENT

This research was supported by a grant from BMW (Bayerische Motoren Werke) AG (Award Number 014806 to the University of California at Berkeley). We are also grateful to Delphine Cody, Avery Jutkowitz, and Christopher Nowakowski for their assistance.

REFERENCES

Anon (1976). Vehicle dynamics terminology, SAE J670e.

Biezad, D.J. (1999). *Integrated Navigation & Guidance Systems*. American Institute of Aeronautics and Astronautics.

Cossalter, V., Da Lio, M., Lot, R., and Fabbri, L. (1999). A general method for the evaluation of vehicle maneuverability with special emphasis on motorcycles. *Vehicle System Dynamics*, **31**, 113–135.

El-Rabbany, A. (2002) *Introduction to GPS*. Artech House.

Fajans, K. (2000). Steering in bicycles and motorcycles. *American Journal of Physics*, **68**(7), 654–659.

Farrell, J. and Barth, M. (1999). The *Global Positioning System and Inertial Navigation*. McGraw-Hill.

Farrell, J., Givargis, T., and Barth, M. (2000) Real time differential carrier phase GPS-aided INS. *IEEE Transactions on Control Systems Technology*, **8**(4), 709–721.

Goodman, L. and Robinson, A. (1952). Effect of finite rotations on gyroscopic sensing devices. *ASME Journal of Applied Mechanics*, **25**, 210–213.

Heckermann, E., Roche, G., and Dance, F. (1997). The BMW on-board navigation system. *SAE Paper Number* 97264025.

Jutkowitz, A. (2003). *On Inertial Navigation of a Motorcycle Using a Limited Number of Sensors*. Master of Science Report, University of California at Berkeley.

Kao, W. (1991). Integration of GPS and dead-reckoning navigation systems. Vehicle Navigation & Information Systems Conference Proceedings. Reprinted as *SAE Paper Number* 912808.

Kessler, P. (2004). *Motorcycle Navigation Using Two Sensors*. Master of Science Report, University of California at Berkeley.

Marsden, J. and Ratiu, T. (1994). *Introduction to Mechanics and Symmetry*. Springer-Verlag.

McGuan, S. (1993). Active human surrogate control of a motorcycle: Stabilizing and de-stabilizing. *SAE Paper Number* 930226.

O'Donnell, C. (1964). *Inertial Navigation – Analysis and Design*. McGraw-Hill Book Company.

O'Reilly, O.M. (1997). On the computation of relative rotations and geometric phases in the motions of rigid bodies. *ASME Journal of Applied Mechanics*, **64**(4), 969–974.

Sharp, R. (1971). The stability and control of motorcycles. *Journal of Mechanical Engineering Science*, **13**(5), 316–329.

Sharp, R. (1985). The lateral dynamics of motorcycles and bicycles. *Vehicle System Dynamics*, **14**(4–6), 265–283.

Sharp, R. (2001). Stability, control, and steering responses of motorcycles. *Vehicle System Dynamics*, **35**(4–5), 291–318.

Sharp, R. and Limebeer, D. (2001). A motorcycle model for stability and control analysis. *Multibody System Dynamics*, **6**, 123–142.

Stevens, B. and Lewis, F. (1992). *Aircraft Control and Simulation*. John Wiley & Sons, Inc.

Stevens, D. (2002). *The Influence of Roll Dynamics on Motorcycle Navigation Systems*. Master of Science Report, University of California at Berkeley.

https://doi.org/10.1017/S037346330500336X Published online by Cambridge University Press

Turetzky, G., Chansarkar, M., and Gehue, H. (1998). GPS as the primary navigation sensor for ITS. *Navigation and Intelligent Transportation Systems*, (R.K. Jurgen, editor), SAE.

Weir, D. (1973). *Motorcycle Handling Dynamics and Rider Control and the Effect of Design Configuration on Response and Performance*. PhD thesis, University of California at Los Angeles.

Weir, D. and Zellner, J. (1978). Advanced motorcycle handling and dynamics. Vol.1- Summary technical report. National Highway Traffic Safety Administration.

Yang, Y. and Farrell, J. (2003). Two antennas GPS-aided INS for attitude determination. *IEEE Transactions on Control Systems Technology*, **11**(6), 905–918.

Zellner, J. and Weir, D. (1978). Development of handling test procedures for motorcycles. *SAE Paper Number* 780313.

https://doi.org/10.1017/S037346330500336X Published online by Cambridge University Press